

# Long-time Freeness in the Kicked Top

Elisa Vallini<sup>1</sup> and Silvia Pappalardi<sup>1</sup>

<sup>1</sup>*Institut für Theoretische Physik, Universität zu Köln, Zùlpicher Straße 77, 50937 Köln, Germany*  
(Dated: November 20, 2024)

Recent work highlighted the importance of higher-order correlations in quantum dynamics for a deeper understanding of quantum chaos and thermalization. The full Eigenstate Thermalization Hypothesis, the framework encompassing correlations, can be formalized using the language of Free Probability theory. In this context, chaotic dynamics at long times are proposed to lead to free independence or “freeness” of observables. In this work, we investigate these issues in a paradigmatic semiclassical model – the kicked top – which exhibits a transition from integrability to chaos. Despite its simplicity, we identify several non-trivial features. By numerically studying  $2n$ -point out-of-time-order correlators, we show that in the fully chaotic regime, long-time freeness is reached exponentially fast. These considerations lead us to introduce a *large deviation theory for freeness* that enables us to define and analyze the associated time scale. The numerical results confirm the existence of a hierarchy of different time scales, indicating a multifractal approach to freeness in this model. Our findings provide novel insights into the long-time behavior of chaotic dynamics and may have broader implications for the study of many-body quantum dynamics.

## I. INTRODUCTION

The study of quantum chaos and the mechanisms by which isolated quantum systems approach thermal equilibrium has fundamentally reshaped our understanding of quantum theory. Recently, attention has shifted toward more refined probes of chaos, with a particular focus on the role of *higher-order correlations* in quantum dynamics. This shift is motivated by developments at the intersection of various fields. In quantum information theory, higher-order moments play a crucial role in  $n$ -designs, ensembles of unitaries that approximate the statistical properties of uniformly random unitaries up to the  $n$ -th moment [1–3]. This framework has inspired the study of thermalization through higher moments of state ensembles, such as those generated via time evolution or projected ensembles [4–13]. New insights into the correlation properties of time-evolved states have also been achieved recently by studies on the statistics of energy eigenstates [14–20].

Concurrently, multi-time correlation functions of physical observables  $\hat{A}$  have gained prominence for their importance in higher-order hydrodynamics beyond the linear response regime [21–24] or for the study of quantum information scrambling, quantified by out-of-time-order correlators (OTOCs)  $\langle \hat{A}(t)\hat{A}\hat{A}(t)\hat{A} \rangle$  [25–28]. These correlators, which involve unconventional time orderings between times, are known to provide insights into quantum chaos that go beyond standard two-time correlators. For example, in the case of underlying chaotic semi-classical dynamics, the OTOCs encode the quantum Lyapunov exponent at short intermediate times [29, 30]. To address properties among  $2n$  times, the so-called  $2n$ -OTOCs

$$\langle (\hat{A}(t)\hat{A})^n \rangle, \quad (1)$$

have been intensively studied [31–35]. These account for  $n$ -designs information [31], and may encode the generalized quantum Lyapunov exponents [36–38].

The established framework for understanding quantum dynamics of observables  $\hat{A}$  is the Eigenstate Thermalization Hypothesis (ETH) [39–41]. ETH assumes that matrix elements of  $\hat{A}$  in the energy eigenbasis look like pseudorandom matrices with smooth statistical properties. To describe multi-time correlation functions such as in Eq. (1), a complete version of ETH has been introduced, named *full ETH*, which encompasses correlations among the matrix elements [42]. The significance of these correlations has attracted substantial interest across fields [43–58]. A recent development in this area has been the formalization of full ETH using Free Probability Theory [59]. Free probability is an extension of traditional probability theory to non-commuting variables [60–62], which introduces powerful tools for understanding the statistical properties of large matrices, such as those that arise in chaotic quantum systems. Originating in planar field theory [63–65], free probability has also played a role in describing correlations in other branches of many-body physics, such as quantum information theory [66], tensor networks [67–70], disordered systems [71–76], and gravity [77–81]. The connection between ETH and free probability provides a mathematical structure to describe correlations through non-crossing partitions, and the so-called free cumulants, connected correlation functions that generalize classical cumulants. In particular, free cumulants between observables at  $2n$  times, i.e.  $\kappa_{2n}(t, 0, \dots, t, 0)$ , provide a means to systematically study the  $2n$ -OTOC in Eq. (1). This approach leads to the proposal that chaotic dynamics shall result at long times in “free independence” or *freeness of observables*, which suggests that observables become statistically independent in a specific, non-classical sense as the system evolves over time [56, 82]. While these ideas are mathematically appealing, their application has been primarily explored in systems evolving with random Wigner matrices [82] or in fine-tuned models, such as dual-unitary circuits [83]. The physical implications of long-time freeness in

realistic chaotic systems remain largely unexplored.

In this work, we address the emergence of freeness at long times by investigating the kicked top, a paradigmatic semiclassical model of quantum chaos [84, 85]. The kicked top describes a system of spins driven periodically in time via collective interactions. Thanks to the latter, the system has a well-defined classical limit, corresponding to the thermodynamic limit, and the dimension of the Hilbert space scales only linearly with the system size, which makes it amenable to exact numerics. Furthermore, this model exhibits a transition from integrability to chaos, making it an ideal setting for investigating the interplay between chaotic dynamics, freeness and its breakdown. Despite its simplicity, the kicked top captures many essential features of chaotic quantum systems, allowing us to identify several features that apply to many-body non-integrable systems.

Let us summarize here our main findings:

- **Emergence of freeness in the chaotic regime**

By investigating numerically the free cumulants, *we demonstrate the emergence of asymptotic freeness at long-times in the chaotic regime* of the kicked top. In contrast to integrable and mixed phase-space regions, where free cumulants saturate to a non-zero value, in the chaotic regime they reach a value that vanishes with the inverse of the size of the Hilbert space  $D$ , i.e.

$$\kappa_{2n}(t, 0, \dots, t, 0) \sim \mathcal{O}(D^{-1}), \quad t \gg 1.$$

This provides direct evidence for the asymptotic long-time freeness of observables. In this regime, *the long-time dynamics of the 2n-point out-of-time-order correlators are governed by free cumulants*. In particular, we find at long-times

$$\langle (\hat{A}_0(t)\hat{A}_0)^n \rangle \simeq \kappa_{2n}(t, 0, \dots, t, 0),$$

where  $\hat{A}_0$  is a traceless observable. Furthermore, at long times, *free cumulants decay exponentially fast* for this class of models.

In the chaotic regime, we further explicitly show that the  $2n$ -OTOC are encoded by ETH-free cumulants (defined below), which account for the matrix elements correlations. We also show that the ETH-free cumulants describe the leading dynamics of the square-commutator, but in this semiclassical model, they fail to reproduce its earliest time behavior, which encodes the Lyapunov exponent.

- **Large Deviation Theory of Freeness** For systems with exponentially decaying free cumulants, we develop a *large deviation approach to freeness*, inspired by standard approaches to multifractality in turbulence [86, 87], chaos theory [88, 89],

and wavefunction localizations [90–92]. When the  $2n$ -OTOCs decay exponentially, one can define a “freeness time-scale” through the quantities  $\tau_n$ , obtained as

$$\langle (\hat{A}_0(t)\hat{A}_0)^n \rangle \sim \exp\left(-\frac{n}{\tau_n}t\right).$$

$\tau_n$  are indicators to quantify how fast freeness at order  $n$  is reached. Under a large deviation assumption, we show that these quantities shall increase monotonically with  $n$  and that they shall be larger than a typical value, i.e.

$$\tau_n \geq \tau_{\text{typ}}.$$

If the times are all equal, it would indicate the absence of fluctuations and a sort of *monofractal behavior*. On the other hand, if the freeness time-scale changes with  $n$ , this implies a *multifractal structure* of the approach to freeness.

We apply this large deviation perspective to the kicked top, where our numerical results reveal a hierarchy of freeness time-scale  $\tau_n$  that increases with  $n$ , indicating a multifractal behavior of the approach to freeness in this generic low-dimensional model of quantum chaos. We also observe the presence of a shift in time of the  $2n$ -OTOC only for even  $n$ , related to the existence of a “Lyapunov regime” for this class of models.

The rest of the paper is structured as follows. In Section II we recall the model of the kicked top and we introduce the main concepts of Free Probability - free cumulants and freeness - connected to the full Eigenstate Thermalization Hypothesis. In Section III, we focus on the dynamics of free cumulants; we observe the emergence of long-time freeness only in the chaotic regime and we highlight the relevance of free cumulants for describing specific correlators like the  $2n$ -OTOCs and the square-commutator. In Section IV, we present the definition of a time scale for the onset of freeness, developing a large deviation theory for freeness in Section IV A. Finally, in Section IV B, we study numerically the freeness time-scale, showing freeness multifractality in the model analyzed. At last, Section V is devoted to the conclusions and the open questions.

## II. MODELING CHAOS: KICKED TOP, FULL ETH AND FREE PROBABILITY

In this section, we recall the definition of the quantum kicked top and we provide a pedagogical review of the Free Probability approach to the full Eigenstate Thermalization Hypothesis, which we will examine in the subsequent analysis. Readers who are familiar with these topics may proceed directly to our results in Sec. III and Sec. IV.

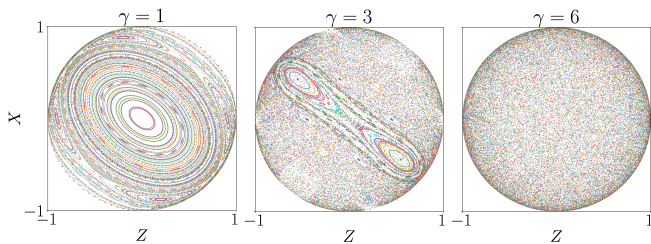


FIG. 1: Transition between regular and chaotic regimes for the classical kicked top. The classical variable is the rescaled angular momentum  $(X, Y, Z) \equiv 2(J_x, J_y, J_z)/N$  which lies on a unitary sphere. Here 253 random initial conditions with  $Y_0 > 0$  are evolved for 250 kicks through the classical equations of motion<sup>1</sup>.

### A. Kicked Top

As a paradigmatic example of semiclassical chaos, we consider a driven system: the kicked top. It is an ensemble of  $N$  spins  $1/2$ , which is driven periodically in time via collective interactions as

$$\hat{H}(t) = p\hat{J}_y + \frac{\gamma}{N}\hat{J}_z^2 \sum_{n=-\infty}^{\infty} \delta(t - \tau n), \quad (2)$$

where  $\hat{J}_i$  is the collective angular momentum operator in the direction  $i = x, y, z$ , i.e.  $[\hat{J}_i, \hat{J}_j] = i\epsilon_{ijk}\hat{J}_k$ . The parameter  $p$  expresses the precession of the collective spin around the  $y$  axis, and  $\gamma$  represents the kicking strength. It is convenient to restrict the discussion to the total symmetric subspace, preserved by the dynamics. The latter is characterized by maximum total angular momentum  $j = N/2$ , fixing the Hilbert space dimension to  $D = N + 1$ . Here  $\tau$  is the period of the periodic kick, which is set to  $\tau = 1$ .

The time evolution operator over one period is the Floquet operator

$$\hat{U}_F = e^{-\frac{i\gamma}{N}\hat{J}_z^2} e^{-ip\hat{J}_y} = \sum_{\alpha} e^{-i\nu_{\alpha}} |\nu_{\alpha}\rangle \langle \nu_{\alpha}|, \quad (3)$$

whose spectrum is given by the Floquet quasi-energies  $\{\nu_{\alpha}\}$ , which are  $2\pi$  periodic; the choice  $\nu_{\alpha} \in [-\pi, \pi)$ ,  $\forall \alpha$  is made.

The quantum system is characterized by a well-defined classical limit obtained for the Planck effective constant

$$\hbar_{\text{eff}} = \frac{\hbar}{N/2}$$

going to zero. Throughout the work, we set  $\hbar = 1$  such that the thermodynamic limit  $N \rightarrow \infty$  corresponds to the semiclassical one.

By increasing the kicking strength  $\gamma$ , the system undergoes a transition between regular and chaotic dynamics: the periodic drive introduces energy into the system, making it chaotic. See Fig. 1 for an illustration of the

classical phase-space for different  $\gamma$ . Being a paradigmatic model of quantum chaos, the classical [84, 85] and quantum [93, 94] features of this transition have been extensively studied, including its OTOC dynamics [95–99].

### B. Free Probability in chaotic dynamics

Here, we introduce the full Eigenstate Thermalization Hypothesis and the Free Probability tools - free cumulants and freeness - which can be applied to multi-time correlation functions. Since we study a periodically driven system, we will concentrate on the description of Floquet systems, which possess a constant density of states. Thus, we will use equilibrium infinite-temperature averages

$$\langle \bullet \rangle = \frac{\text{tr}(\bullet)}{D},$$

where  $D$  is the dimension of the Hilbert space, and focuses on the quasi-energy eigenbasis. For discussions involving the energy eigenstates, as well as canonical and microcanonical averages, we refer the reader to Refs. [56–59].

#### 1. Full Eigenstate Thermalization Hypothesis

According to the Eigenstate Thermalization Hypothesis [39–41], the matrix elements  $A_{\alpha\beta} = \langle \nu_{\alpha} | \hat{A} | \nu_{\beta} \rangle$  of a physical observable  $\hat{A}$  in the quasi-energy eigenbasis behave as pseudorandom matrix with smooth statistical properties. The full ETH [42] extends the standard formulation to multiple-point correlations between matrix elements. Specifically, statistical averages<sup>2</sup> of products with distinct indices  $\alpha_1 \neq \alpha_2 \neq \dots \neq \alpha_n$  read

$$\overline{A_{\alpha_1\alpha_2} A_{\alpha_2\alpha_3} \dots A_{\alpha_n\alpha_1}} = D^{1-n} F^{(n)}(\omega_{\alpha_1\alpha_2}, \dots, \omega_{\alpha_{n-1}\alpha_n}) \quad (4a)$$

<sup>1</sup> The stroboscopic classical evolution is given by the following:

$$\begin{aligned} X' &= (X \cos p + Z \sin p) \cos(\gamma Z') - Y \sin(\gamma Z') \\ Y' &= (X \cos p + Z \sin p) \sin(\gamma Z') + Y \cos(\gamma Z') \\ Z' &= Z \cos p - X \sin p. \end{aligned}$$

<sup>2</sup> Although matrix elements are completely determined by the eigenvectors of a fixed Hamiltonian, they behave pseudorandomly, and the statistical average shall be intended over a “fictitious ensemble” that can be defined heuristically in several ways, such as averaging over a small window of energies or adding a small disordered term to the Hamiltonian and averaging over it, see e.g. [42, 100]. In practice, the average shall be valid “typically” and ETH can be understood as a self-averaging property of matrix elements.

where  $F^{(n)}$  are some smooth functions of the eigenenergies differences  $\omega_{\alpha_1\alpha_2} = \nu_{\alpha_1} - \nu_{\alpha_2}$  that define the observable. For  $n = 1, 2$  one recovers the standard ETH [40], where in the Floquet basis  $F^{(1)} = \langle \hat{A} \rangle$  is the constant equilibrium average and  $F^{(2)}(\omega) = |f(\omega)|^2$  is the dynamical correlation function. When indices are repeated, the average of the products factorizes at the leading order in  $D$  as

$$\begin{aligned} & \overline{A_{\alpha_1\alpha_2} \dots A_{\alpha_{m-1}\alpha_1} A_{\alpha_1\alpha_{m+1}} \dots A_{\alpha_n\alpha_1}} \quad (4b) \\ &= \overline{A_{\alpha_1\alpha_2} \dots A_{\alpha_{m-1}\alpha_1}} \overline{A_{\alpha_1\alpha_{m+1}} \dots A_{\alpha_n\alpha_1}} + \mathcal{O}(D^{-1}). \end{aligned}$$

The full ETH ansatz is needed to study equilibrium multi-time correlation functions, where products of many-matrix elements naturally appear, i.e.

$$\langle \hat{A}(t_1) \dots \hat{A}(t_n) \rangle = \frac{1}{D} \sum_{\alpha_1, \dots, \alpha_n} e^{i\vec{\omega} \cdot \vec{t}} A_{\alpha_1\alpha_2} \dots A_{\alpha_n\alpha_1} \quad (5)$$

$$\text{with } \vec{\omega} = (\omega_{\alpha_1\alpha_2}, \dots, \omega_{\alpha_n\alpha_1}), \quad \vec{t} = (t_1, \dots, t_n)$$

As a result of the smoothness of the matrix elements and of the scaling with  $D$  in Eq. (4), Ref. [42] showed that the correlation functions at each  $n$  are organized in terms of sums over distinct indices as

$$\mathcal{K}_n(\vec{t}) := \frac{1}{D} \sum_{\alpha_1 \neq \dots \neq \alpha_n} e^{i\vec{\omega} \cdot \vec{t}} A_{\alpha_1\alpha_2} \dots A_{\alpha_n\alpha_1}. \quad (6)$$

These are referred to as *ETH simple loops* because, in the diagrammatic representations of the full ETH, they correspond to diagrams where energy indices appear as dots arranged in a single loop. For completeness, a detailed discussion of ETH diagrams and the derivation of this result is provided in App. A. Furthermore, according to Eq. (4a), the simple loops can be written as

$$\mathcal{K}_n(\vec{t}) = \int d\vec{\omega} e^{i\vec{\omega} \cdot \vec{t}} F^{(n)}(\vec{\omega}),$$

which states that ETH smooth functions are linked to the Fourier Transform of  $\mathcal{K}_n(\vec{t})$ . In summary, *within ETH the building blocks of multi-time correlations are given by simple loops  $\mathcal{K}_n(\vec{t})$ .*

## 2. Free Cumulants

The simple loops  $\mathcal{K}_n$  in Eq. (6) appearing in ETH description of multi-time correlators can actually be identified as *free cumulants*, a familiar object in the theory of Free Probability [62], see Refs. [101, 102] for an introduction.

Free cumulants  $\kappa_n$  are connected correlation functions defined from moments of  $n$  variables. Let us here consider the case of a time-dependent observable at different times:  $\hat{A}(t_i)$   $i = 1, \dots, n$ . Free cumulants are defined implicitly and recursively through the moments-free cumulant formula [62]:

$$\langle \hat{A}(t_1) \dots \hat{A}(t_n) \rangle = \sum_{\pi \in NC(n)} \kappa_\pi(\hat{A}(t_1), \dots, \hat{A}(t_n)), \quad (7)$$

where  $\pi \in NC(n)$  are noncrossing partitions of a set of  $n$  elements. The  $\kappa_\pi$  is the product of free cumulants, one for each block  $B$  of the partition, based on the number of elements of the block, i.e.

$$\kappa_\pi(\hat{A}(t_1), \dots, \hat{A}(t_n)) = \prod_{B \in \pi} \kappa_{|B|} \left( \prod_{q=1}^{|B|} \hat{A}(t_q) \right),$$

where  $q$  counts the number of terms in each block from 1 to its length  $|B|$ . As an example, the first free cumulants for equal-times observables  $\hat{A}(t_i) = \hat{A}$  are defined by

$$\begin{aligned} \langle \hat{A} \rangle &= \kappa_1 \\ \langle \hat{A}^2 \rangle &= \kappa_2 + \kappa_1^2 \\ \langle \hat{A}^3 \rangle &= \kappa_3 + \kappa_1^3 + 3\kappa_1\kappa_2 \\ \langle \hat{A}^4 \rangle &= \kappa_4 + \kappa_1^4 + 6\kappa_1^2\kappa_2 + 4\kappa_1\kappa_3 + 2\kappa_2^2 \end{aligned} \quad (8)$$

with the notation  $\kappa_n \equiv \kappa_n(\hat{A}, \dots, \hat{A})$ .<sup>3</sup>

While Eq. (7) is just an implicit definition of free cumulants in terms of moments, when ETH applies, the *free cumulants correspond to the ETH simple loops  $\mathcal{K}_n$*  defined in Eq. (6) namely [59]

$$\kappa_n(\hat{A}(t_1), \dots, \hat{A}(t_n)) = \mathcal{K}_n(\vec{t}) + \mathcal{O}(D^{-1}). \quad (9)$$

This follows from the ETH properties (1,2) discussed in App. A, which show that multi-time correlations have exactly the combinatorics of noncrossing partitions and that they can be rewritten only in terms of simple loops. In the example of  $n = 4$ , the free cumulants are defined through Eq. (8), while the expression of the equal-time correlation function through ETH is given in Fig. 10 in the App. A; these two formulas have the same structure. This can be generalized  $\forall n$ , allowing the identification of free cumulants  $\kappa_n$  with ETH simple loops  $\mathcal{K}_n$ , from now on called *ETH-free cumulants*. Therefore, free probability provides the combinatorics needed for the calculation of multi-time correlations, when ETH is applied.

## 3. Freeness

A central concept in Free Probability is free independence, or *freeness*, which generalizes the classical notion of independence from commuting to non-commuting variables. Two large  $D \times D$  matrices  $A$  and  $B$  are said to be

<sup>3</sup> The definition is based on the combinatorial aspects of partitions of a set of  $n$  elements; in the same way as the classical cumulants are related to the lattice of all partitions, free cumulants are related only to the lattice of noncrossing partitions. In the example (8), cumulants for the classical theory of probability would have been defined in the same way apart from  $\langle A^4 \rangle_{cl} = \langle A^4 \rangle + \kappa_2^2$ , for the contribution of one crossing partition (there are no crossing partitions for  $n < 4$ ).



asymptotically free if their mixed free cumulants (defined in Eq. (7)) vanish  $\forall n$ :

$$\kappa_{2n}(A, B, \dots) = 0, \quad (10)$$

where ‘‘asymptotically’’ indicates that this condition holds as the matrix dimension  $D$  diverges. When  $A$  and  $B$  are free, their mixed moments can be computed from their individual moments only<sup>4</sup>. The mixed moments admit a compact expression given by [103]

$$\langle (AB)^n \rangle = \sum_{\pi \in NC(n)} \kappa_{\pi}(A, \dots, A) \langle B^n \rangle_{\pi^*}, \quad (11)$$

where  $\langle B^n \rangle_{\pi^*}$  is the product of moments, one for each term of the partition  $\pi^*$ , known as the Kraweras complement (or dual) of the partition  $\pi$ <sup>5</sup>.

If the vanishing of free cumulants in Eq. (10) holds only up to a certain order  $n$ , then  $A$  and  $B$  are termed *asymptotically  $n$ -free*. Important examples of free variables can be found in random matrix theory [60, 103], specifically when considering randomly rotated deterministic matrices  $B$  and  $A^U = U^\dagger A U$ . When  $U$  is sampled from the Haar ensemble,  $A^U$  and  $B$  are asymptotically free [103]. If  $U$  is sampled from an  $n$ -design (an ensemble of unitaries that approximates the Haar measure up to order  $n$ ), then  $A^U$  and  $B$  are asymptotically  $n$ -free [23].

Notably, chaotic time evolution leads to arbitrary asymptotically  $n$ -freeness of physical observables at long-times, in the limit of diverging system sizes. While this holds for random matrices [82], it can also be derived for generic many-body Hamiltonians as a consequence of the Eigenstate Thermalization Hypothesis [56]. For quantum observables  $\hat{A}(t)$  and  $\hat{B}$  satisfying ETH, the infinite-time average of their mixed free cumulants vanishes:

$$\lim_{T \rightarrow \infty} \frac{1}{T} \int_0^T dt \kappa_{2n}(\hat{A}(t), \hat{B}, \dots) = 0.$$

<sup>4</sup> For example, consider the implicit definition in Eq. (7) for alternating free variables  $A, B$ :

$$\begin{aligned} \langle AB \rangle &= \kappa_1(A)\kappa_1(B) + \kappa_2(A, B) \quad \text{with} \quad \kappa_2(A, B) = 0 \\ \rightarrow \langle AB \rangle &= \langle A \rangle \langle B \rangle, \end{aligned}$$

$$\begin{aligned} \langle ABAB \rangle &= \kappa_4(A, B, A, B) + \kappa_1^2(A)\kappa_1^2(B) + 4\kappa_1(A)\kappa_1(B)\kappa_2(A, B) \\ &\quad + \kappa_1^2(A)\kappa_2(B) + \kappa_1^2(B)\kappa_2(A) \\ &\quad + 2\kappa_1(A)\kappa_3(B, A, B) + 2\kappa_1(B)\kappa_3(A, B, A) \\ &\quad + 2\kappa_2^2(A, B) \quad \text{with} \quad \kappa_n(A, B, \dots) = 0 \\ \rightarrow \langle ABAB \rangle &= (\langle A^2 \rangle - \langle A \rangle^2) \langle B^2 \rangle + \langle A \rangle^2 \langle B^2 \rangle. \end{aligned}$$

<sup>5</sup> The Kraweras complement  $\pi^*$  of a partition  $\pi$  is defined by the property that the blocks composing  $\pi^*$  are the maximal blocks (polygons) with vertices on ‘‘ $B$ ’’ that do not cross the blocks of  $\pi$ .

This result is derived using i) the ETH, which expresses free cumulants as sums of simple loops, and ii) a no-resonance condition between eigenvalues<sup>6</sup>, believed to hold generically in non-integrable systems [40, 104]. This suggests that chaotic time evolution at infinite times is as effective as an  $n$ -design in inducing freeness among observables.

The infinite-time average serves as a mathematical tool, but in a physical system, it is conjectured that asymptotically  $n$ -freeness is reached at a finite time. One of the goals of this work is to properly define the time scale associated with freeness, which generically depends on  $n$  and that shall quantify how fast freeness is achieved. In a finite system with finite Hilbert space dimension  $D$ ,  $n$ -freeness is expected to emerge at long-times with a  $\mathcal{O}(D^{-1})$  correction, as

$$\kappa_{2n}(\hat{A}(t), \hat{B}, \dots) \approx \mathcal{O}(D^{-1}), \quad \text{for } t \gg 1. \quad (12)$$

Long-time freeness implies that mixed moments at late times can be computed using established properties of Free Probability [103] such as the factorization of Eq. (11). This can be directly applied to out-of-time order correlators. For instance, the OTOC between  $\hat{A}(t)$  and  $\hat{B}$  at long-times  $t \gg 1$  is given by:

$$\langle \hat{A}(t) \hat{B} \hat{A}(t) \hat{B} \rangle = \kappa_2(\hat{A}, \hat{A}) \langle \hat{B} \rangle^2 + \langle \hat{A} \rangle^2 \langle \hat{B}^2 \rangle + \mathcal{O}(D^{-1}). \quad (13)$$

In the case of traceless observables  $\langle \hat{A} \rangle = \langle \hat{B} \rangle = 0$ , this quantity vanishes as  $\mathcal{O}(D^{-1})$ .

In this work, we focus on probing freeness through the study of *free cumulants of out-of-time order alternating operators* such as

$$\kappa_{2n}(t, 0, \dots, t, 0) \equiv \kappa_{2n}(\hat{A}(t), \hat{A}, \dots, \hat{A}(t), \hat{A}).$$

This choice is motivated by the fact that they are related to  $2n$ -OTOC and that they exhibit the slowest dynamics and, consequently, determine the freeness scale at order  $n$ . In general, the calculation of the free cumulants follows from the recursive definition in Eq. (7). To simplify the calculations, we will often consider traceless observables, i.e.

$$\hat{A}_0 = \hat{A} - \langle \hat{A} \rangle \mathbf{I}, \quad (14)$$

in order to have  $\kappa_1(\hat{A}_0) = \langle \hat{A}_0 \rangle = 0$ . The free cumulants of  $\hat{A}_0$  can be recursively computed starting from

<sup>6</sup> The ETH free cumulant in Eq. (9) is given by sums of simple loops over distinct indices. Hence its time-average selects only terms satisfying  $\sum_{i=1}^m E_{\alpha_i} = \sum_{i=1}^m E_{\beta_i}$ , where  $m$  indicates the number of times that  $\hat{A}(t)$  and  $\hat{B}$  are alternating. The non-resonance condition implies that such equality is satisfied only if the set  $\{\alpha_i\}$  is a permutation of the set  $\{\beta_i\}$ . Since the sum is only over distinct indices, this implies that the time average vanishes.

$\kappa_1(\hat{A}_0) = \langle \hat{A}_0 \rangle = 0$ , as

$$\kappa_2(t, 0) = \langle \hat{A}_0(t) \hat{A}_0 \rangle, \quad (15a)$$

$$\kappa_3(t, 0, t) = \langle \hat{A}_0(t) \hat{A}_0 \hat{A}_0(t) \rangle, \quad (15b)$$

$$\begin{aligned} \kappa_4(t, 0, t, 0) &= \langle \hat{A}_0(t) \hat{A}_0 \hat{A}_0(t) \hat{A}_0 \rangle \\ &\quad - 2\kappa_2^2(t, 0), \end{aligned} \quad (15c)$$

$$\begin{aligned} \kappa_5(t, 0, t, 0, t) &= \langle \hat{A}_0(t) \hat{A}_0 \hat{A}_0(t) \hat{A}_0 \hat{A}_0(t) \rangle \\ &\quad - 5\kappa_2(t, 0)\kappa_3(t, 0, t), \end{aligned} \quad (15d)$$

$$\begin{aligned} \kappa_6(t, 0, t, 0, t, 0) &= \langle \hat{A}_0(t) \hat{A}_0 \hat{A}_0(t) \hat{A}_0 \hat{A}_0(t) \hat{A}_0 \rangle \\ &\quad - 5\kappa_2^3(t, 0) + 3\kappa_3^2(t, 0, t) \\ &\quad - 6\kappa_2(t, 0)\kappa_4(t, 0, t, 0), \end{aligned} \quad (15e)$$

and so on.

### III. FREE CUMULANTS DYNAMICS

Let us now present our results for the dynamics of alternating free cumulants in the kicked-top model.

To study the dynamics at stroboscopic times, we perform an exact diagonalization of the Floquet operator given in Eq. (3), with the parameter fixed at  $p = 4\pi/7$ . Since the Hamiltonian in Eq. (2) is invariant under  $\pi$ -rotations around the  $y$ -axis, we restrict our analysis to the positive-parity subspace, which has a dimension of  $D = N/2 + 1$ . For concreteness, we focus on the dynamics of the observable

$$\hat{A} = \frac{\hat{J}_y^2}{(N/2)^2}, \quad (16)$$

which has a finite average of  $\kappa_1 = \langle \hat{A} \rangle = 1/3 + \mathcal{O}(D^{-1})$ . We have confirmed that the qualitative behavior of our results is robust to this choice of observable.

We begin by discussing long-time freeness in the regular, mixed and chaotic regimes (Sec. III A). Secondly, we focus on the chaotic limit and we show that the dynamics at long times of  $2n$ -OTOCs of traceless observables is given only by the highest-order free cumulant  $\kappa_{2n}(t, 0, \dots, t, 0)$  (Sec. III B). Finally, we confirm the validity of ETH in the chaotic regime, showing explicitly the decomposition of multi-time correlation functions in ETH-free cumulants; moreover, we pinpoint the inadequacy of the ETH prediction when it comes to describing the early-time behavior of the square-commutator (Sec. III C).

#### A. Long-time freeness and chaos

We find that long-time freeness is achieved only in the regime associated with full chaos in the classical limit. This is evident already at the level of the fourth-free cumulant  $\kappa_4(t, 0, t, 0)$ , expected to vanish in

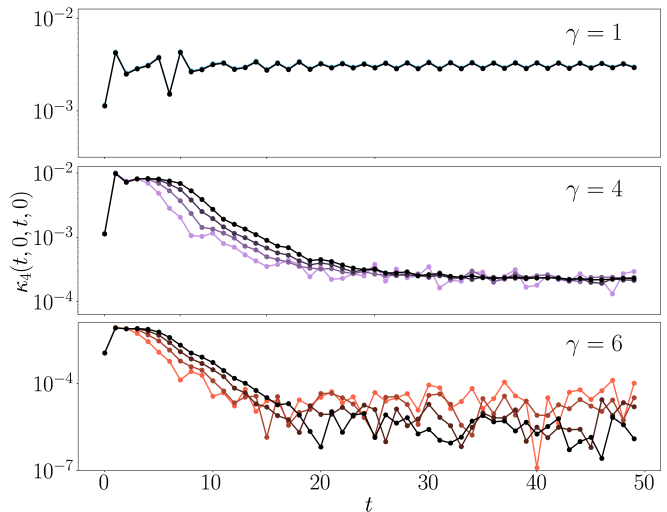


FIG. 2: Evolution in time of  $\kappa_4(t, 0, t, 0)$  for the traceless observable  $\hat{A}_0$  obtained from  $\hat{A}$  in Eq. (16), for the kicked top (2). Three regimes are displayed: regular for  $\gamma = 1$  in the upper panel, mixed for  $\gamma = 4$  in the central panel and fully chaotic for  $\gamma = 6$  in the bottom panel. In every panel, different system sizes are shown ( $N \in [600, 1400, 3000, 6000]$ , from light to dark colors).

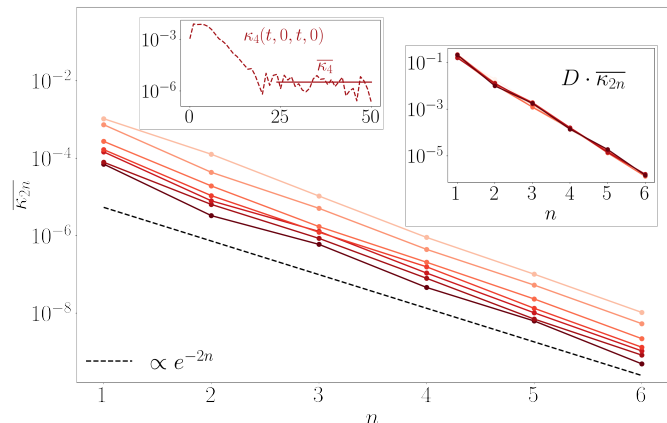


FIG. 3: Saturation value at long-times of the free cumulants in the chaotic case  $\gamma = 6$ , as a function of  $n$ , for different system sizes ( $N \in [300, 600, 1400, 2000, 3000, 4000, 6000]$ , from light to dark colors).  $\overline{\kappa_{2n}}$  is obtained averaging  $\kappa_{2n}(t, 0, \dots, t, 0)$  between  $t = 25$  and  $t = 50$  as shown in the inset on the left, for  $n = 2$ . They are calculated for the traceless observable  $\hat{A}_0$  obtained from  $\hat{A}$  in Eq. (16), for the kicked top (2).

the presence of asymptotic freeness for large  $D$ , as  $\kappa_4(t, 0, t, 0) \sim \mathcal{O}(D^{-1})$ . In Fig. 2, we report the numerical evaluation of the free cumulant, calculated using Eq. (15c), for different system sizes across three regimes: regular (upper panel,  $\gamma = 1$ ), mixed (center panel,  $\gamma = 4$ ), and fully chaotic (bottom panel,  $\gamma = 6$ ).

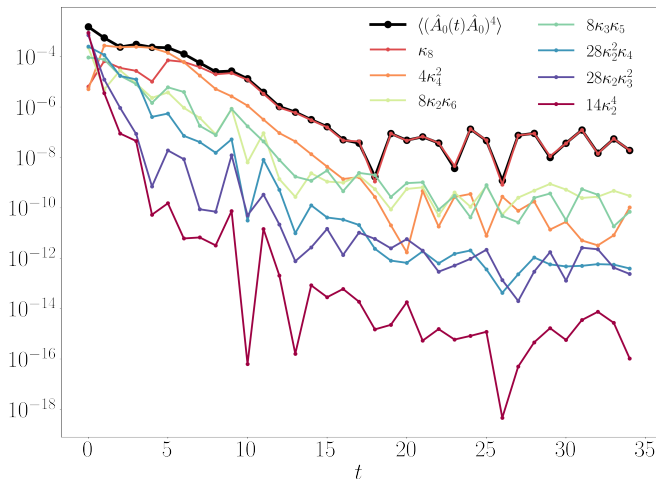


FIG. 4: Dynamics of the 8-OTOC compared with the free cumulants in which it can be rewritten (Eq. (18)). The traceless observable  $\hat{A}_0$  is obtained from  $\hat{A}$  in Eq. (16), for the kicked top (2) in the chaotic case  $\gamma = 6$ , for  $N = 6000$ .

The data show that in the regular and mixed phase-space regimes, the saturation value remains constant with increasing system size, indicating the absence of long-time freeness. In contrast, for  $\gamma = 6$ , at long times the free cumulant fluctuates around a value that decreases as the Hilbert space dimensionality  $D$  increases, as predicted by Eq. (12) for  $\hat{B} = \hat{A}(0)$ . The absence of late-time freeness in the regular and mixed phase-space can be attributed to the failure of the Eigenstate Thermalization Hypothesis, which is instead satisfied in the chaotic regime, as we discuss in more detail in Sec. III C.

To quantitatively characterize the emergence of freeness in the chaotic regime, we focus on  $\gamma = 6$ , and we analyze the long-time saturation value of the free cumulants  $\kappa_{2n}(t, 0, \dots, t, 0)$  as  $n$  and the system size  $D$  are changed. We compute the exact time evolution, using Eq. (15), up to  $n = 6$ . In Fig. 3 we consider the time-average  $\overline{\kappa_{2n}}$ , obtained averaging  $\kappa_{2n}(t, 0, \dots, t, 0)$  over time, between  $t = 25$  and  $t = 50$ . Free cumulants saturate to a value that vanishes as  $D^{-1}$ , as encoded in Eq. (12). This is a known feature characterizing long-time dynamics of out-of-time ordered correlators [105]. In the case of free cumulants as well, this value stems from the fluctuations of matrix elements, and as such, it is not presently captured by the full ETH in Eqs. (4). The data show that the plateau is also decreasing with the order of the power  $n$ , proportionally to  $e^{-2n}$ . Overall, we find

$$\overline{\kappa_{2n}} \sim \frac{e^{-2n}}{D} \quad (17)$$

After the saturation to  $1/D$ , one may eventually expect signatures of level repulsion at even longer time scales, see e.g. Ref. [32, 34]. A more detailed understanding of this phenomenon is left to future investigation.

## B. Free cumulants and $2n$ out-of-time order correlators

Free cumulants play a crucial role in the dynamics of the  $2n$ -out-of-time order correlation  $\langle\langle \hat{A}(t)\hat{A}^n \rangle\rangle$ , as shown in Refs. [57, 106] for the standard OTOC at  $n = 2$ . We will now discuss it for an arbitrary order of  $n$ . In particular, we focus on the case  $n = 4$ , but the same results have been obtained for different values of  $n$ . We consider  $2n$ -OTOCs of traceless observables, as in Eq. (14), computed via Eq. (15). We will restore the effect of a finite first moment in Sec. III C below. Having traceless operators  $\langle \hat{A}_0 \rangle = 0$  implies that the  $2n$ -OTOCs should asymptotically vanish to zero over a long-time since the time-independent plateau has been shifted to zero, see the right-end side of Eq. (13).

In Fig. 4, we compare the evolution of the 8-OTOC, with the various free cumulants of  $\hat{A}_0$  which appear in its decomposition, namely

$$\begin{aligned} \langle\langle \hat{A}_0(t)\hat{A}_0^4 \rangle\rangle &= \kappa_8(t, 0, \dots, t, 0) + 4\kappa_4^2(t, 0, t, 0) + \\ &+ 8\kappa_6(t, 0, t, 0, t, 0)\kappa_2(t, 0) + \kappa_5(t, 0, t, 0, t)\kappa_3(t, 0, t) + \\ &+ 28\kappa_2^2(t, 0)\kappa_4(t, 0, t, 0) + 28\kappa_2(t, 0)\kappa_3^2(t, 0, t) + \\ &+ 14\kappa_2^4(t, 0). \end{aligned} \quad (18)$$

We observe that at long times, the evolution of the 8-OTOC is given only by  $\kappa_8(t, 0, \dots, t, 0)$ , while the other contributions decay to zero more rapidly. In other words, the higher free cumulant constitutes the slowest contribution to the  $2n$ -OTOC and one can identify the two as

$$\langle\langle \hat{A}_0(t)\hat{A}_0^n \rangle\rangle \sim \kappa_{2n}(t, 0, \dots, t, 0) \quad \text{for } t \gg 1. \quad (19)$$

At long times, where the free cumulants saturate to a plateau, this feature is compatible with the scaling observed in Eq. (17). Products of  $\alpha$  free cumulants scale as  $D^{-\alpha}$ . Hence, the only contribution scaling as  $D^{-1}$  is given by  $\kappa_{2n}$ , which dominates over the other terms and gives the total saturation of the  $2n$ -OTOC.

Eq. (19) is also valid in the intermediate regime, where, furthermore, the numerical results in Fig. 4 show that for this model freeness is reached exponentially fast

$$\langle\langle \hat{A}_0(t)\hat{A}_0^n \rangle\rangle \sim \kappa_{2n}(t, 0, \dots, t, 0) \sim \exp\left(-\frac{n}{\tau_n}t\right).$$

The quantities  $\tau_n$  so defined,

$$\frac{1}{\tau_n} = -\frac{1}{nt} \log \left| \langle\langle \hat{A}_0(t)\hat{A}_0^n \rangle\rangle \right| \quad \text{for } t \gg 1, \quad (20)$$

indicate how quickly freeness is achieved and can be referred as definition of a *freeness time-scale*. We note that standard 4-OTOC was already found to decay exponentially fast after the Ehrenfest time in quantum systems with a few-body chaotic limits, see e.g. Refs.[107, 108]. The goal of Sec. IV will be to interpret the decay rate for arbitrary  $n$  in a general way, from a large deviation theory.

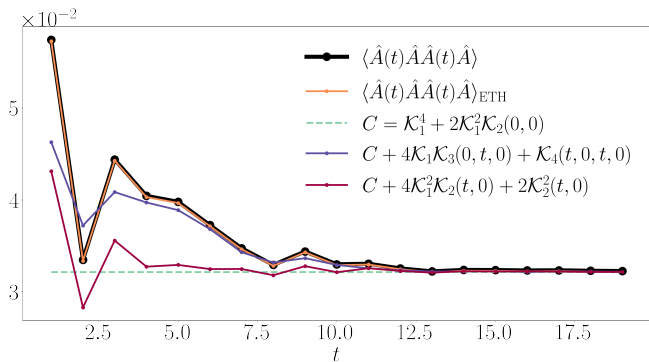


FIG. 5: Dynamics of the OTOC in Eq. (21) compared with the one calculated through the ETH decomposition in Eq. (22). The contributions from different free cumulants are displayed with different colours. The observable chosen is  $\hat{A}$  in Eq. (16), for the kicked top (2) in the chaotic case  $\gamma = 6$ , for  $N = 6000$ .

### C. ETH-free cumulants in the chaotic regime

At the beginning of this section, we stated that freeness is achieved in the chaotic regime as a result of the validity of the Eigenstate Thermalization Hypothesis. Focusing on the regime for  $\gamma = 6$ , we now demonstrate how the correlations from ETH serve as the fundamental building blocks for multi-time correlators in the large  $N$  limit. For this purpose, we will consider the evolution of the observable  $\hat{A}$  in Eq. (16) which possesses finite average  $\kappa_1 = \langle \hat{A} \rangle \simeq 1/3$ .

*OTOC decomposition and ETH-free cumulants* We start by showing that the building blocks of the dynamics are given by the ETH simple loops, in other words, that the free cumulants correspond at the leading order to sums over different indices, as stated in Eq. (9), that is

$$\kappa_n(t, 0, \dots, t, 0) = \mathcal{K}_n(t, 0, \dots, t, 0) + \mathcal{O}(D^{-1}).$$

We study the exact dynamics of the out-of-time order correlator

$$\langle \hat{A}(t) \hat{A} \hat{A}(t) \hat{A} \rangle = \frac{1}{D} \sum_{i,j,k,l} e^{i(\omega_{ij} + \omega_{kl})t} A_{ij} A_{jk} A_{kl} A_{li}, \quad (21)$$

and contrast it with the prediction obtained via ETH, namely:

$$\begin{aligned} \langle \hat{A}(t) \hat{A} \hat{A}(t) \hat{A} \rangle_{\text{ETH}} &= \mathcal{K}_4(t, 0, t, 0) + \mathcal{K}_1^4 + 4\mathcal{K}_1^2 \mathcal{K}_2(t, 0) + \\ &+ 2\mathcal{K}_1^2 \mathcal{K}_2(0, 0) + 4\mathcal{K}_1 \mathcal{K}_3(0, t, 0) + \\ &+ 2\mathcal{K}_2^2(t, 0), \end{aligned} \quad (22)$$

where we recall that  $\mathcal{K}_n$  are the ETH simple loops given by sums over different indices as in Eq. (6). In particular,

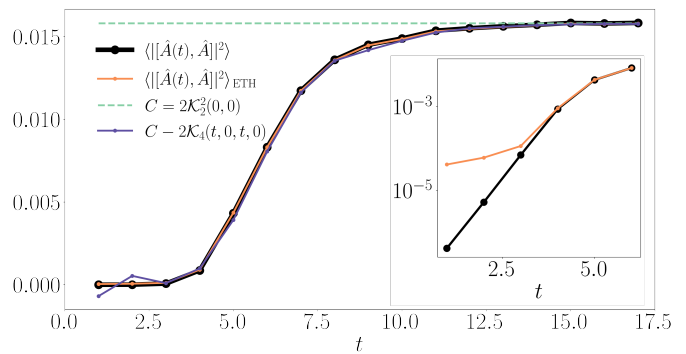


FIG. 6: Exact dynamics of the square-commutator in Eq. (23) (black line) is compared with the ETH approximation in Eq. (26) (orange line). The dashed green line indicates the time-independent plateau, while the violet line shows the contribution due to the ETH-free cumulant  $\mathcal{K}_4$ . In the inset, we show the same data in a logarithmic scale at short times. The observable chosen is  $\hat{A}$  in Eq. (16), for the kicked top (2) in the chaotic case  $\gamma = 6$ , for  $N = 6000$ .

one has  $\mathcal{K}_1 = \kappa_1$ . In Fig. 5, we plot the exact result (21) and the ETH prediction (22) for  $N = 6000$ , which shows an excellent agreement, confirming the validity of full ETH in the chaotic regime.

We note that while  $\mathcal{K}_2(t, 0)$  decays rapidly to zero, the dynamics of the OTOC are dictated mostly by high-order connected correlation functions and, in particular, by the fourth-free cumulant, namely

$$\langle \hat{A}(t) \hat{A} \hat{A}(t) \hat{A} \rangle \simeq C + \mathcal{K}_4(t, 0, t, 0).$$

This also shows that the late-time behavior of the OTOC is encoded in  $\mathcal{K}_4(t, 0, t, 0)$ ; as we saw above, this feature is generic and applies to arbitrary  $2n$ -OTOCs.

At long times, the OTOC approaches a plateau given only by the time-independent contributions since the time-dependent free cumulants decrease to zero, displaying freeness. The value of the plateau  $C = \mathcal{K}_1^4 + 2\mathcal{K}_1^2 \mathcal{K}_2(0, 0)$  corresponds to the one predicted by Free Probability for free-variables in Eq. (13) for  $\hat{B} = \hat{A}$ , i.e.

$$C = \mathcal{K}_1^2 \langle \hat{A}^2 \rangle + \mathcal{K}_1^2 \mathcal{K}_2.$$

*Square-commutator and ETH free cumulants* We now show that free cumulants play a crucial role also in describing the dynamics of the so-called square-commutator, defined as

$$\langle [|\hat{A}(t), \hat{A}|]^2 \rangle = -2\langle \hat{A}(t) \hat{A} \hat{A}(t) \hat{A} \rangle + 2\langle \hat{A}^2(t) \hat{A}^2 \rangle, \quad (23)$$

which contains, in turn, out-of-time order correlators. In systems with a well-defined classical chaotic limit, this object grows as [29, 30]

$$\langle [|\hat{A}(t), \hat{A}|]^2 \rangle \sim \hbar_{\text{eff}}^2 e^{2\tilde{\lambda}t}, \quad (24)$$



until the Ehrenfest time (also called scrambling time)

$$t_{\text{Ehr}} \sim \log h_{\text{eff}}^{-1} / \tilde{\lambda} \quad (25)$$

in the limit  $h_{\text{eff}} \rightarrow 0$ . Beyond this time, quantum effects become significant, causing the square-commutator to saturate. The rate  $\tilde{\lambda}$  is often referred to as the quantum Lyapunov exponent [25–28].

We now explore how well the ETH predictions apply to Eq. (23). In the chaotic regime the square-commutator can be decomposed in terms of ETH-free cumulants as follows

$$\begin{aligned} \langle |[\hat{A}(t), \hat{A}]|^2 \rangle_{\text{ETH}} &= -2\mathcal{K}_4(t, 0, t, 0) + 2\mathcal{K}_4(t, t, 0, 0) \\ &\quad - 2\mathcal{K}_2^2(t, 0) + 2\mathcal{K}_2^2(0, 0), \end{aligned} \quad (26)$$

where the OTOC in Eq. (23) is expanded as in Eq. (22), and the time-ordered correlator is factorized as<sup>7</sup>

$$\begin{aligned} \langle \hat{A}^2(t) \hat{A}^2 \rangle_{\text{ETH}} &= \mathcal{K}_4(t, t, 0, 0) + \mathcal{K}_1^4 + 4\mathcal{K}_1^2 \mathcal{K}_2(t, 0) \\ &\quad + 2\mathcal{K}_1^2 \mathcal{K}_2(0, 0) + 4\mathcal{K}_1 \mathcal{K}_3(0, t, 0) \\ &\quad + \mathcal{K}_2^2(0, 0) + \mathcal{K}_2^2(t, 0). \end{aligned}$$

In Fig. 6, we compare the numerical results of the exact square-commutator with its ETH-free cumulants decomposition from Eq. (26), which shows very good agreement. By examining the individual free cumulants, a clear hierarchy emerges in their contributions to the square-commutator dynamics: i)  $\mathcal{K}_2^2(0, 0)$  determines the saturation value, being the only time-independent free cumulant, which serves as yet another manifestation of freeness; ii)  $\mathcal{K}_2^2(t, 0)$  and  $\mathcal{K}_4(t, t, 0, 0)$  decay rapidly and fluctuate around zero; iii)  $\mathcal{K}_4(t, 0, t, 0)$  drives much of the distinguishing dynamics of the square-commutator, particularly the evolution towards the plateau. Since this term encodes correlations among different matrix elements, the results confirm the idea of ascribing the peculiar dynamics of the square-commutator to the ETH correlations (see, e.g., Ref. [42]).

However, we note that the ETH alone is insufficient to fully capture the behavior of the square-commutator at *very early times*, as shown in the inset of Fig. 6. While the square-commutator initially grows as  $h_{\text{eff}}^2 \sim D^{-2}$ , the ETH decomposition is valid only at  $\mathcal{O}(D^{-1})$ , leading to a parametric discrepancy between the two curves in the early-time regime. Therefore, for this class of models, the early-time exponential growth is not solely captured by  $\mathcal{K}_4(t, 0, t, 0)$ , but rather involves subleading terms from both crossing loops and the decomposition of noncrossing terms. This calls for a better understanding of the subleading contributions and higher-order correction to the full ETH.

In conclusion, even if the ETH-free cumulants fail to reproduce the earliest dynamics, the numerical data show that the behavior of the square-commutator is predominantly governed by the  $\mathcal{K}_4(t, 0, t, 0)$  cumulant, stemming from the OTOC.

#### IV. TIME SCALE FOR THE ONSET OF FREENESS

In Section III B we demonstrated that both  $2n$ -OTOCs and  $2n$ -free cumulants exhibit exponential decay in reaching long-time freeness, in the kicked-top model, meaning

$$\langle (\hat{A}_0(t) \hat{A}_0)^n \rangle \sim \exp\left(-\frac{n}{\tau_n} t\right) \quad \text{for } t \gg 1. \quad (27)$$

The quantities  $\tau_n$  quantify how quickly freeness is achieved. Building on these findings, we develop a large deviation framework (Sec. IV A) to understand this time scale, followed by a numerical analysis (Sec. IV B) in the context of the kicked-top model.

##### A. Large Deviation Theory for Freeness

We consider generic  $2n$ -OTOCs of traceless observables that decay exponentially as

$$\langle (\hat{A}_0(t) \hat{A}_0)^n \rangle \sim e^{-R_n t} \quad \text{for } t \gg 1, \quad (28)$$

where for illustration purposes, we used  $R_n = n/\tau_n$ . The  $2n$ -OTOC are moments of order  $n$  of the spectrum of the operator

$$\begin{aligned} \hat{A}_0(t) \hat{A}_0 &= \sum_i g_i(t) |i_t\rangle \langle i_t|, \\ \text{with } g_i(t) &= G_i e^{-\rho_i(t)t} e^{i\theta_i(t)} \end{aligned} \quad (29)$$

where  $g_i(t)$  are complex eigenvalues, with  $e^{-\rho_i(t)t}$  representing the time-dependent part of the modulus  $|g_i(t)|$ . In a generic system, the decay rates  $\rho_i(t)$  are distributed and fluctuate over time. Therefore, probing their higher moments through  $2n$ -OTOCs provides insight into their dynamical distribution.

To describe their temporal fluctuations, we take inspiration from studies in multifractality, turbulence, and chaos [86–92]. After defining the probability distribution of the decay rates as  $P(\rho_t) = \frac{1}{D} \sum_i^D \delta(\rho_t - \rho_i(t))$ , we assume the existence of a typical value  $\rho_{\text{typ}}$  and a Large Deviation form at long-times for it:

$$P(\rho_t) \propto e^{\Gamma(\rho_t)t} \quad \text{for } t \gg 1, \quad (30)$$

where  $\Gamma(\rho_t)$  is analogous to the Cramér function in large deviation theory, it is concave and has its maximum at

<sup>7</sup> This decomposition highlights how certain ETH diagrams (see App. A), initially distinct between the two correlators before applying ETH, factorize in the same way for large system sizes. They thus cancel out at the leading order and give only subleading contributions to Eq. (26).

the typical value where it also vanishes, i.e.,  $\Gamma(\rho_{\text{typ}}) = 0$  and  $\Gamma'(\rho_t)|_{\rho_{\text{typ}}} = 0$ . We now demonstrate that assuming a large deviation principle for the spectrum of this operator yields specific properties for  $\tau_n$ .

Indeed, from Eq. (30) we can derive the exponential time-decay:

$$\begin{aligned} \langle (\hat{A}_0(t)\hat{A}_0)^n \rangle &= \frac{1}{D} \sum_i G_i^n e^{-n\rho_i(t)t} e^{in\theta_i} \\ &\propto \int_{\rho_{\min}}^{\rho_{\max}} d\rho e^{-(n\rho - \Gamma(\rho))t} \approx e^{-\text{Min}_\rho(n\rho - \Gamma(\rho))t}, \end{aligned} \quad (31)$$

where the integral on the right-end side is solved using that, for  $t \gg 1$ , the dominant contribution comes from the inferior stationary point of the exponent function. Comparing Eq. (31) with Eq. (28) we get that

$$R_n = \text{Min}_\rho(n\rho - \Gamma(\rho)) \quad (32)$$

is a Legendre transform of  $\Gamma(\rho)$ ; as a consequence, since  $\Gamma$  is a concave function of  $\rho$ ,  $R_n$  is also a concave function of  $n$ . Not only,  $R_n/n$  decreases monotonically with  $n$ , leading to the inequality

$$R_n \leq n\rho_{\text{typ}},$$

where the typical value  $\rho_{\text{typ}}$  is given by

$$\rho_{\text{typ}} = \lim_{n \rightarrow 0} \frac{R_n}{n} = \left. \frac{\partial R_n}{\partial n} \right|_{n=0}. \quad (33)$$

Coming back to the times  $\tau_n = n/R_n$ , it follows that they are monotonically increasing with  $n$ , and, setting  $\tau_{\text{typ}} = \rho_{\text{typ}}^{-1}$ , they satisfy

$$\tau_n \geq \tau_{\text{typ}}. \quad (34)$$

Let us discuss some physical consequences. The decay rate of the  $2n$ -free cumulants (or equivalently, the  $2n$ -OTOCs of traceless observables) quantifies how quickly freeness emerges and can be viewed as a probe for the temporal fluctuations in the spectrum of time-dependent observables. The freeness time-scale  $\tau_n$ , defined in Eq. (20), capture the average decay of these moments and provide a meaningful description of the dynamical fluctuations, incorporating finite-time properties.

In the limit where fluctuations are absent<sup>8</sup>, we find  $\tau_n = \tau_{\text{typ}}$ . Analogous to studies of fractal dimensions in chaotic systems, systems exhibiting this property can be referred to as *monofractal*. However, in general, we shall expect that the freeness time-scale  $\tau_n$  will depend on  $n$ , implying a *multifractal* structure in the approach to freeness.

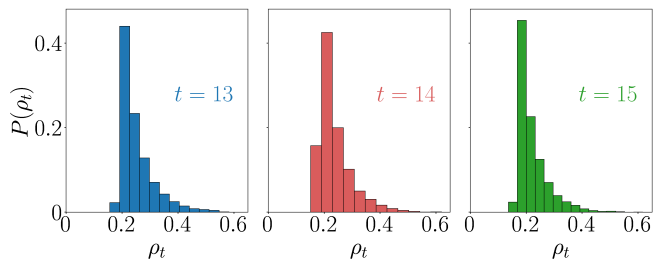


FIG. 7: Probability distribution  $P(\rho_t)$  for the decay rates evaluated as  $-\log |g_i(t)|/t$ , for  $t = 13, 14, 15$ , from the spectrum of  $\hat{A}_0(t)\hat{A}_0$  (see Eq. (29)). The traceless observable  $\hat{A}_0$  is obtained from  $\hat{A}$  in Eq. (16), for the kicked top (2) in the chaotic case  $\gamma = 6$ , for  $N = 6000$ .

## B. Freeness multifractality in the Kicked Top

Let us now turn to the numerical study of the onset of freeness in the chaotic regime of the kicked top.

We have tested numerically that the large deviation ansatz in Eq. (30) is satisfied. In Fig. 7 we show the probability distribution  $P(\rho_t)$  for the decay rates  $\rho_i(t)$  defined in Eq. (29), evaluated as  $-\log |g_i(t)|/t$ , for  $t = 13, 14, 15$ . The distribution is compatible with the large deviation ansatz in Eq. (30): it gives rise to a concave exponent function that does not change in time and it is centered around a specific time-independent value  $\rho_{\text{typ}}$ .

We now report the detailed study of the freeness time-scale  $\tau_n$  as defined from Eq. (20). We study the exact dynamics of free-cumulants computed using Eq. (15). In Fig. 8 we plot the rescaled  $2n$ -OTOC

$$\frac{1}{n} \log \left| \langle (\hat{A}_0(t)\hat{A}_0)^n \rangle \right|$$

for  $n = 1, 2, 3, 4$ , from left to right. The plot shows that the  $2n$ -OTOCs decay exponentially fast in time, according to Eq. (27) (linear decay in this scale). The data suggest that freeness is slower for increasing order  $n$ , as predicted by our large deviation theory in the case of multifractal behavior.

To quantitatively address this issue, we evaluate the freeness time-scale  $\tau_n$  by performing linear fits on the curves shown in Fig. 8, for  $N = 6000$ . These fits are conducted within an intermediate regime, which is selected by omitting the initial time steps and extending up to the point where the plateau is reached.

We show  $\tau_n$  as a function of  $n$  in the inset of Fig. 8 (right-end panel), up to  $n = 6$  (the dynamics for  $n = 5, 6$  is not shown). The data shows that  $\tau_n$  is a monotonic increasing function of  $n$ , thus confirming the expected behavior from the large deviation theory presented above, cf. Eq. (34).

As discussed in Sec. III A above, at longer times, the  $2n$ -OTOCs display fluctuations around a plateau  $\mathcal{O}(D^{-1})$  indicating freeness.

<sup>8</sup> This holds if the probability distribution in Eq. (30) is  $P(\rho) \propto \delta(\rho - \rho_{\text{typ}})$ .

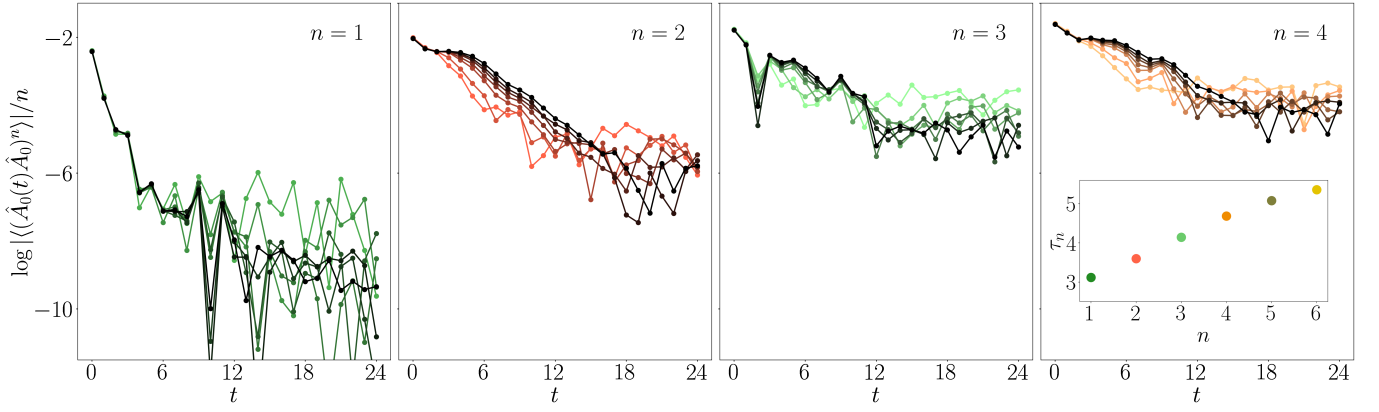


FIG. 8: The quantity  $\log |\langle (\hat{A}_0(t)\hat{A}_0)^n \rangle|/n$  as a function of time for different  $n$ , from left to right  $n = 1, 2, 3, 4$ . In each figure, the system size is increased as  $N \in [300, 600, 1400, 3000, 4000, 6000]$ , from light to dark colors. In the inset the freeness time-scale  $\tau_n$  as a function of  $n$ , obtained through linear fits of the curves in an intermediate regime, for  $N = 6000$ . The traceless observable  $\hat{A}_0$  is obtained from  $\hat{A}$  in Eq. (16), for the kicked top (2) in the chaotic case  $\gamma = 6$ .

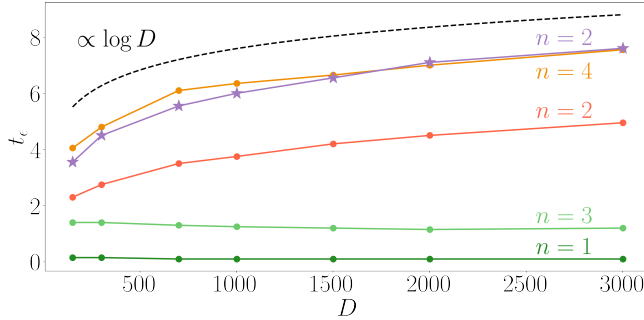


FIG. 9:  $t_\epsilon$  defined as the first interpolated time for which  $\frac{1}{n} \log |\langle (\hat{A}_0(t)\hat{A}_0)^n \rangle| < \epsilon = -2.55$  as a function of the  $n$  system size, for different  $n$ . Points markers indicate the chaotic case  $\gamma = 6$ ; the colors refer to the associated curves in Fig. 8. The purple-star curve, instead, indicates the case  $\gamma = 4$ , referring to Fig. 2. The traceless observable  $\hat{A}_0$  is obtained from  $\hat{A}$  in Eq. (16), for the kicked top (2).

From Fig. 8, we also highlight a qualitative difference between even and odd powers. In the case of *even*  $n$ , the  $2n$ -OTOC display a *time shift*, which grows logarithmically with the system size.

This is shown in Fig. 9, where we plot the time  $t_\epsilon$  at which each  $2n$ -OTOC reaches an  $\epsilon$  value, as a way to quantify the shift. For definiteness, we fix  $\epsilon = -2.55$  and calculate  $t_\epsilon$  as the first interpolated time for which  $\log |\langle (\hat{A}_0(t)\hat{A}_0)^n \rangle|/n \leq \epsilon$ , for  $n = 1, 2, 3, 4$ . The data show a clear logarithmic increase of  $t_\epsilon$  for even  $n$ , while the time is constant for odd  $n$ . Furthermore, we also note that the time shift depends on the amount of chaos present in the system. We calculate the time shift also for  $\gamma = 4$  and  $n = 2$  corresponding to the mixed phase-

space region discussed, see e.g. Fig. 2 in Sec. III A. In this case, the time shift  $t_\epsilon$  is bigger than the corresponding one for  $\gamma = 6$ , indicating a smaller shift for more chaotic systems.

In the case of models with a semiclassical chaotic limit  $\hbar_{\text{eff}} \rightarrow 0$ , the explanation for this effect can be found in the early-time dynamics of the  $2n$ -OTOCs. This behavior has been studied for few-body quantum chaos [107, 108], as well as for the Sachdev-Ye-Kitaev (SYK) model [109], for  $n = 2$ . In this case, the OTOC is known to have a Lyapunov regime at short intermediate times, meaning it is governed by the exponential growth of the square-commutator (cf. Eq. (24)). In particular,

$$\langle \hat{A}(t)\hat{A}\hat{A}(t)\hat{A} \rangle \sim \text{const.} - e^{2\tilde{\lambda}(t-t_{\text{Ehr}})} \quad (35a)$$

for  $1 \ll t \ll t_{\text{Ehr}}$ , with the Ehrenfest time defined in Eq. (25). After this time the square-commutator saturates.

For higher and even  $n = 2m$ , a similar behavior to the one of Eq. (35a) is conjectured to be valid at short intermediate times [36], i.e.

$$\langle (\hat{A}(t)\hat{A})^{2m} \rangle \sim \text{const.} - e^{L_{2m}(t-t_{\text{Ehr}}^{(2m)})} \quad (35b)$$

for  $1 \ll t \ll t_{\text{Ehr}}^{(2m)}$ , where  $L_{2m}$  are the rates accounted by the so-called generalized Lyapunov exponents, which stem from the powers of the square-commutator  $\langle |[\hat{A}(t), \hat{A}(0)]|^{2m} \rangle \sim \hbar_{\text{eff}}^{2m} e^{L_{2m}t}$ . One retrieves the square commutator for  $m = 1$  ( $n = 2$ ). This behavior is valid until the generalized Ehrenfest time  $t_{\text{Ehr}}^{(2m)} \sim \log \hbar_{\text{eff}}^{-2m}/L_{2m}$ , which is assumed to be increasing with  $m$ , see also Refs.[37, 38]. After this time scale, the higher powers of the square-commutator saturate. In the case of odd powers, this effect is not present, indeed, the odd powers of the commutator usually do not have exponential growth due to a cancellation of signs.

As a consequence, the behavior described in Eq. (35b) holds up to  $t_{\text{Ehr}}^{(2m)}$ , which marks the saturation of higher powers of the square-commutator and correspondingly the initial point after which the  $4m$ -OTOC exhibits the exponential decay. Since for this model  $\hbar_{\text{eff}}^{-1} \sim D$ , this leads to

$$t_{\text{shift}}^{(2m)} \sim t_{\text{Ehr}}^{(2m)} \sim \frac{2m}{L_{2m}} \log D .$$

In summary, the observed time shift is explained through the Ehrenfest time: the exponential decay of the  $4m$ -OTOCs starts later for bigger  $D$ , and it is inversely proportional to the amount of chaos, thus explaining the results in Fig. 9.

## V. CONCLUSIONS AND DISCUSSION

In this work, we explored the emergence of long-time freeness induced by chaotic dynamics in the kicked top, a prototypical model of few-body quantum chaos. We established that long-time freeness is reached exponentially fast in the chaotic regime. This led us to introduce a large deviation theory for the approach to freeness and the associated time scale.

Our results indicate that Free Probability could have a wider range of applicability in the study of many-body quantum systems. We conclude with a discussion of potential future directions stemming from this work, which would be valuable to explore.

- *Large deviation theory of freeness.* Guided by approaches in turbulence, chaos, and eigenstate delocalization, in this work, we introduced a large deviation theory of freeness, which shall apply generically to exponentially decaying  $2n$ -OTOCs. The associated freeness time-scale  $\tau_n$  describe the time-dependent fluctuations of the spectrum of time-evolving observables and indicate a multifractal behavior if  $\tau_n > \tau_{\text{typ}}$  dependent on  $n$ , and a form of monofractality if  $\tau_n = \tau_{\text{typ}}$  for every  $n$ . In quantum systems with a few-body classical chaotic limits, the exponential decay of the 4-OTOC was interpreted from the point of view of mixing and associated with Ruelle-Pollicot resonances by Refs.[107, 108], see also Ref. [110]. Within this framework, it would be intriguing to explore whether the mono/multifractal behaviors in the large deviation theory of freeness can be interpreted in terms of these resonances.

Although our analysis stems from chaos in few-body semiclassical systems, it should extend to any context where freeness is achieved exponentially, including many-body systems. For example, recent findings report exponential decay in free cumulants of order  $n$  within dual-unitary circuits [83], suggesting promising directions for future exploration of the freeness time-scale in many-body settings.

Another potential future direction would amount to exploring the effects of locality in the large deviation theory of freeness, leading to questions also about the (potentially  $n$ -dependent) butterfly velocity and its behavior in local systems, such as clean or random circuits.

- *Beyond full ETH.* Throughout this work, we have focused on expectation values, whose leading behavior is well described by ETH-free cumulants. However, ETH predictions are accurate only at the leading order and do not fully account for subleading effects, which appear at order  $\mathcal{O}(D^{-1})$ .

For instance, we have shown that the leading-order ETH predictions fail to capture the early-time behavior of the square-commutator (see Sec. III C) or the late-time fluctuations of the free cumulants (see Sec. III A). This highlights the need to extend ETH to account for finite system size corrections.

Finally, we explored the development of freeness and free-cumulant dynamics up to their  $\mathcal{O}(1/D)$  saturation level. At even longer time scales, signatures of level repulsion may appear. This effect is known at the level of the two-point function [111–115], and it is also expected at higher orders [32, 34]. While this is consistent with asymptotic long-time freeness, it invites further investigation into how higher-order spectral fluctuations manifest in observable quantities.

## ACKNOWLEDGEMENTS

We thank X. Turkeshi, B. Pain and J. Kudler-Flam for their insightful discussions, L. Foini for valuable feedback on our work, and J. Kurchan for collaboration on related projects. We acknowledge support by the Deutsche Forschungsgemeinschaft (DFG, German Research Foundation) under Germany's Excellence Strategy - Cluster of Excellence Matter and Light for Quantum Computing (ML4Q) EXC 2004/1 -390534769, and DFG Collaborative Research Center (CRC) 183 Project No. 277101999 - project B02.

## Appendix A: Diagrammatic representation of the Full Eigenstate Thermalization Hypothesis

The full Eigenstate Thermalization Hypothesis ansatz in Eq. (4) can be represented in a pictorial way via *ETH diagrams*; the product of  $n$  matrix elements is drawn as a loop with  $n$  dots, where every dot indicates an index and every arc of the circle between two consecutive dots refers to the matrix element with the related indices. By convention, the factors of the product are written down clockwise along the loop, starting from the upper dot. In the presence of repeated indices, lines are drawn to connect dots with equal indices. One recognizes three

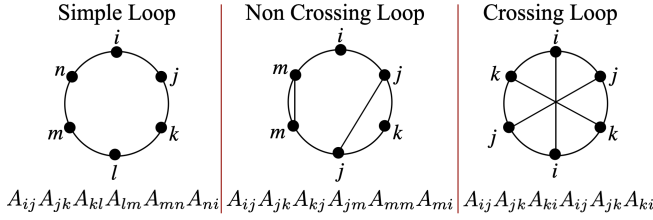


$$\langle \hat{A}^4 \rangle = \sum \text{diagram 1} + \sum \text{diagram 2} + 4 \sum \text{diagram 3} + 2 \sum \text{diagram 4} + 4 \sum \text{diagram 5} + 2 \sum \text{diagram 6} + \sum \text{diagram 7}$$

$$\langle \hat{A}^4 \rangle_{\text{ETH}} = \mathcal{K}_4 + \mathcal{K}_1^4 + 4\mathcal{K}_1^2\mathcal{K}_2 + 2\mathcal{K}_1^2\mathcal{K}_2 + 4\mathcal{K}_1\mathcal{K}_3 + 2\mathcal{K}_2^2$$

FIG. 10: Four-time correlation function. In the first row, pictorial representation: the sum in Eq. (5) for  $n = 4$  has been split in sums over all possible combinations of repeated indices or, in other words, in all the possible ETH diagrams with four dots; the result is made of sums of simple, non crossing and crossing loops. In the second row, simplification, as ETH is applied: non crossing diagrams factorize in simple diagrams whose contribution is given by Eq. (6), whereas the crossing diagram is negligible; thanks to these two conditions,  $\mathcal{K}_n$  are identified as free cumulants, for large  $D$ . Indeed, while the decomposition in the first row is exact, the second one is true at the first order in the system size  $D$ . One diagram and its factorization are indicated with the same color. We mention that some loops have cyclic permutations, indicated by the numbers in front of the sums, which in general lead to free cumulants with different time dependences (here we considered equal-time, for convenience).

different types of diagrams (simple loops, noncrossing, and crossing) based on the drawn lines. Some examples of ETH diagrams for  $n = 6$  are here represented:



The full ETH ansatz permits to study equilibrium multi-time correlation functions, i.e.

$$\langle \hat{A}(t_1) \dots \hat{A}(t_n) \rangle = \frac{1}{D} \sum_{\alpha_1, \dots, \alpha_n} e^{i\vec{\omega} \cdot \vec{t}} A_{\alpha_1 \alpha_2} \dots A_{\alpha_n \alpha_1} \cdot$$

with  $\vec{\omega} = (\omega_{\alpha_1 \alpha_2}, \dots, \omega_{\alpha_n \alpha_1})$ ,  $\vec{t} = (t_1, \dots, t_n)$

We now illustrate how within ETH the building blocks of multi-time correlations are  $\mathcal{K}_n(\vec{t})$  as given in Eq. 6. We start from the sum over all the indices in the correlation: this can be split in one sum with all different indices ( $\sum_{\alpha_1 \neq \dots \neq \alpha_n}$ ) plus sums in which only one index is repeated ( $\sum_{\alpha_1 = \alpha_2 \neq \alpha_3 \neq \dots \neq \alpha_n}$  for instance), plus sums with two repeated indices and so on. In a pictorial fashion, the correlation function is drawn through sums of  $n$ -dots loops with all the possible contractions of lines: a sum over a  $n$ -dots simple loop plus sums over all possible crossing and noncrossing loops (see Fig. 10 for the case  $n = 4$ ). At this level, the ETH diagrams have been used only as bookkeeping; their usefulness arises when one applies the full ETH at the level of each sum:

- the sum of a simple loop is given by

$$\mathcal{K}_n(\vec{t}) := \frac{1}{D} \sum_{\alpha_1 \neq \dots \neq \alpha_n} e^{i\vec{\omega} \cdot \vec{t}} A_{\alpha_1 \alpha_2} \dots A_{\alpha_n \alpha_1} \cdot$$

According to Eq. (4a), this quantity can be written as  $\mathcal{K}_n(\vec{t}) = \int d\vec{\omega} e^{i\vec{\omega} \cdot \vec{t}} F^{(n)}(\vec{\omega})$  which states that

ETH smooth functions are linked to the Fourier Transform of  $\mathcal{K}_n(\vec{t})$ . For instance,

$$\sum \text{diagram 1} = \frac{1}{D} \sum_{i \neq j \neq k \neq l} e^{i(\omega_{ij}t_1 + \omega_{jk}t_2 + \omega_{kl}t_3 + \omega_{li}t_4)} A_{ij}A_{jk}A_{kl}A_{li} = \mathcal{K}_4(t_1, t_2, t_3, t_4);$$

- the sum of a non crossing loop factorizes in the sums of simple loops with lower numbers of dots. For instance, according to Eq. (4b) applied on the product of matrix elements
$$\sum \text{diagram 2} = \frac{1}{D} \sum_{i \neq k \neq l} e^{i(\omega_{ik}t_2 + t_3\omega_{kl} + t_4\omega_{li})} A_{ii}A_{ik}A_{kl}A_{li} = \mathcal{K}_1\mathcal{K}_3(t_2, t_3, t_4) + \mathcal{O}\left(\frac{1}{D}\right) = \sum \text{diagram 3} \sum \text{diagram 4} + \mathcal{O}\left(\frac{1}{D}\right);$$
- the sum of a crossing loop, instead, gives a negligible contribution at the first order in the system size. For instance, according to Eq. (4b) applied on the product of matrix elements
$$\sum \text{diagram 5} = \frac{1}{D} \sum_{i \neq j} e^{i\omega_{ij}(t_1 - t_2 + t_3 - t_4)} (A_{ij}A_{ji})^2 \sim \frac{1}{D}$$
and can therefore be neglected.

Summarizing, the full Eigenstate Thermalization Hypothesis can be reformulated as the *two ETH properties*:

1. suppression of crossing diagrams, e.g.

$$\sum \text{diagram 6} = \frac{1}{D},$$

2. factorization of noncrossing diagrams in simple loops, e.g.

$$\sum \text{diagram 7} = \sum \text{diagram 8} \sum \text{diagram 9},$$

at the leading order in the system size.

Hence, the simplified result for correlations calculated through ETH, for large system sizes, is a sum of products of  $\mathcal{K}_n$  for different  $n$  i.e. diagrams involving only sums over different indices; these building blocks of multi-time

correlations are called plainly “ETH simple loops” in the text. The explicit formula for the case  $n = 4$  is reported in Fig. 10.

- 
- [1] Philippe Delsarte, Jean-Marie Goethals, and Johan Jacob Seidel, “Spherical codes and designs,” in *Geometry and Combinatorics* (Elsevier, 1991) pp. 68–93.
- [2] Christoph Dankert, “Efficient simulation of random quantum states and operators,” [arXiv preprint quant-ph/0512217](#) (2005).
- [3] Christoph Dankert, Richard Cleve, Joseph Emerson, and Etera Livine, “Exact and approximate unitary 2-designs and their application to fidelity estimation,” *Phys. Rev. A* **80**, 012304 (2009).
- [4] Jordan S Cotler, Daniel K Mark, Hsin-Yuan Huang, Felipe Hernandez, Joonhee Choi, Adam L Shaw, Manuel Endres, and Soonwon Choi, “Emergent quantum state designs from individual many-body wave functions,” *PRX Quantum* **4**, 010311 (2023).
- [5] Joonhee Choi, Adam L. Shaw, Ivaylo S. Madjarov, Xin Xie, Ran Finkelstein, Jacob P. Covey, Jordan S. Cotler, Daniel K. Mark, Hsin-Yuan Huang, Anant Kale, Hannes Pichler, Fernando G. S. L. Brandão, Soonwon Choi, and Manuel Endres, “Preparing random states and benchmarking with many-body quantum chaos,” *Nature* **613**, 468–473 (2023).
- [6] Wen Wei Ho and Soonwon Choi, “Exact emergent quantum state designs from quantum chaotic dynamics,” *Phys. Rev. Lett.* **128**, 060601 (2022).
- [7] Pieter W Claeys and Austen Lamacraft, “Emergent quantum state designs and biunitarity in dual-unitary circuit dynamics,” *Quantum* **6**, 738 (2022).
- [8] Matteo Ippoliti and Wen Wei Ho, “Solvable model of deep thermalization with distinct design times,” *Quantum* **6**, 886 (2022).
- [9] Maxime Lucas, Lorenzo Piroli, Jacopo De Nardis, and Andrea De Luca, “Generalized deep thermalization for free fermions,” *Phys. Rev. A* **107**, 032215 (2023).
- [10] Tanmay Bhore, Jean-Yves Desaulles, and Zlatko Papić, “Deep thermalization in constrained quantum systems,” *Phys. Rev. B* **108**, 104317 (2023).
- [11] Max McGinley and Michele Fava, “Shadow tomography from emergent state designs in analog quantum simulators,” *Phys. Rev. Lett.* **131**, 160601 (2023).
- [12] Saúl Pilatowsky-Cameo, Ceren B. Dag, Wen Wei Ho, and Soonwon Choi, “Complete hilbert-space ergodicity in quantum dynamics of generalized fibonacci drives,” *Phys. Rev. Lett.* **131**, 250401 (2023).
- [13] Daniel K Mark, Federica Surace, Andreas Elben, Adam L Shaw, Joonhee Choi, Gil Refael, Manuel Endres, and Soonwon Choi, “A maximum entropy principle in deep thermalization and in hilbert-space ergodicity,” [arXiv preprint arXiv:2403.11970](#) (2024).
- [14] Anatoly Dymarsky, Nima Lashkari, and Hong Liu, “Subsystem eigenstate thermalization hypothesis,” *Phys. Rev. E* **97**, 012140 (2018).
- [15] Yichen Huang, “Universal eigenstate entanglement of chaotic local hamiltonians,” *Nuclear Physics B* **938**, 594–604 (2019).
- [16] Tsung-Cheng Lu and Tarun Grover, “Renyi entropy of chaotic eigenstates,” *Phys. Rev. E* **99**, 032111 (2019).
- [17] Chaitanya Murthy and Mark Srednicki, “Structure of chaotic eigenstates and their entanglement entropy,” *Physical Review E* **100**, 022131 (2019).
- [18] Zhengyan Darius Shi, Shreya Vardhan, and Hong Liu, “Local dynamics and the structure of chaotic eigenstates,” *Physical Review B* **108**, 224305 (2023).
- [19] Dominik Hahn, David J. Luitz, and J. T. Chalker, “Eigenstate correlations, the eigenstate thermalization hypothesis, and quantum information dynamics in chaotic many-body quantum systems,” *Phys. Rev. X* **14**, 031029 (2024).
- [20] Siddharth Jindal and Pavan Hosur, “Generalized free cumulants for quantum chaotic systems,” [arXiv preprint arXiv:2401.13829](#) (2024).
- [21] Benjamin Doyon and Jason Myers, “Fluctuations in ballistic transport from euler hydrodynamics,” in *Annales Henri Poincaré*, Vol. 21 (Springer, 2020) pp. 255–302.
- [22] Jason Myers, Joe Bhaseen, Rosemary J Harris, and Benjamin Doyon, “Transport fluctuations in integrable models out of equilibrium,” *SciPost Physics* **8**, 007 (2020).
- [23] Michele Fava, Sounak Biswas, Sarang Gopalakrishnan, Romain Vasseur, and SA Parameswaran, “Hydrodynamic nonlinear response of interacting integrable systems,” *Proceedings of the National Academy of Sciences* **118**, e2106945118 (2021).
- [24] Luca V Delacrétaz and Ruchira Mishra, “Nonlinear response in diffusive systems,” *SciPost Physics* **16**, 047 (2024).
- [25] Juan Maldacena, Stephen H. Shenker, and Douglas Stanford, “A bound on chaos,” *Journal of High Energy Physics* **2016** (2016).
- [26] Pavan Hosur, Xiao-Liang Qi, Daniel A. Roberts, and Beni Yoshida, “Chaos in quantum channels,” *Journal of High Energy Physics* **2016** (2016).
- [27] Shenglong Xu and Brian Swingle, “Scrambling dynamics and out-of-time ordered correlators in quantum many-body systems: a tutorial,” [arXiv preprint arXiv:2202.07060](#) (2022).
- [28] Ignacio García-Mata, Rodolfo A. Jalabert, and Diego A. Wisniacki, “Out-of-time-order correlators and quantum chaos,” *Scholarpedia* **18**, 55237 (2023), [arXiv:2209.07965 \[quant-ph\]](#).
- [29] AI Larkin and Yu N Ovchinnikov, “Quasiclassical method in the theory of superconductivity,” *Soviet Physics JETP* **28**, 1200–1205 (1969).
- [30] A. Kitaev, *Talk given at the Fundamental Physics Prize Symposium* (20145).
- [31] Daniel A Roberts and Beni Yoshida, “Chaos and complexity by design,” *Journal of High Energy Physics* **2017**, 1–64 (2017).
- [32] Jordan Cotler, Nicholas Hunter-Jones, Junyu Liu, and Beni Yoshida, “Chaos, complexity, and random matrices”

- ces,” *Journal of High Energy Physics* **2017**, 1–60 (2017).
- [33] Naoto Tsuji, Tomohiro Shitara, and Masahito Ueda, “Bound on the exponential growth rate of out-of-time-ordered correlators,” *Physical Review E* **98**, 012216 (2018).
- [34] Jordan Cotler and Nicholas Hunter-Jones, “Spectral decoupling in many-body quantum chaos,” *Journal of High Energy Physics* **2020**, 1–62 (2020).
- [35] Lorenzo Leone, Salvatore FE Oliviero, You Zhou, and Aloscia Hamma, “Quantum chaos is quantum,” *Quantum* **5**, 453 (2021).
- [36] Silvia Pappalardi and Jorge Kurchan, “Quantum bounds on the generalized lyapunov exponents,” *Entropy* **25**, 246 (2023).
- [37] Dmitrii A Trunin, “Quantum chaos without false positives,” *Physical Review D* **108**, L101703 (2023).
- [38] Dmitrii A Trunin, “Refined quantum lyapunov exponents from replica out-of-time-order correlators,” *Physical Review D* **108**, 105023 (2023).
- [39] Mark Srednicki, “Chaos and quantum thermalization,” *Physical Review E* **50**, 888–901 (1994).
- [40] Mark Srednicki, “The approach to thermal equilibrium in quantized chaotic systems,” *Journal of Physics A: Mathematical and General* **32**, 1163–1175 (1999).
- [41] Luca D’Alessio, Yariv Kafri, Anatoli Polkovnikov, and Marcos Rigol, “From quantum chaos and eigenstate thermalization to statistical mechanics and thermodynamics,” *Advances in Physics* **65**, 239–362 (2016).
- [42] Laura Foini and Jorge Kurchan, “Eigenstate thermalization hypothesis and out of time order correlators,” *Phys. Rev. E* **99**, 042139 (2019).
- [43] Tomaz Prosen, “Ergodic properties of a generic nonintegrable quantum many-body system in the thermodynamic limit,” *Phys. Rev. E* **60**, 3949–3968 (1999).
- [44] Julian Sonner and Manuel Vielma, “Eigenstate thermalization in the sachdev-ye-kitaev model,” *Journal of High Energy Physics* **2017**, 1–28 (2017).
- [45] Laura Foini and Jorge Kurchan, “Eigenstate thermalization and rotational invariance in ergodic quantum systems,” *Phys. Rev. Lett.* **123**, 260601 (2019).
- [46] Amos Chan, Andrea De Luca, and J. T. Chalker, “Eigenstate correlations, thermalization, and the butterfly effect,” *Phys. Rev. Lett.* **122**, 220601 (2019).
- [47] Chaitanya Murthy and Mark Srednicki, “Bounds on chaos from the eigenstate thermalization hypothesis,” *Physical Review Letters* **123** (2019).
- [48] Jonas Richter, Anatoly Dymarsky, Robin Steinigeweg, and Jochen Gemmer, “Eigenstate thermalization hypothesis beyond standard indicators: Emergence of random-matrix behavior at small frequencies,” *Physical Review E* **102** (2020).
- [49] Jiaozi Wang, Mats H Lamann, Jonas Richter, Robin Steinigeweg, Anatoly Dymarsky, and Jochen Gemmer, “Eigenstate thermalization hypothesis and its deviations from random-matrix theory beyond the thermalization time,” *arXiv preprint arXiv:2110.04085* (2021).
- [50] Marlon Brenes, Silvia Pappalardi, Mark T. Mitchison, John Goold, and Alessandro Silva, “Out-of-time-order correlations and the fine structure of eigenstate thermalization,” *Physical Review E* **104** (2021).
- [51] Anatoly Dymarsky, “Bound on eigenstate thermalization from transport,” *Phys. Rev. Lett.* **128**, 190601 (2022).
- [52] Zohar Nussinov and Saurish Chakrabarty, “Exact universal chaos, speed limit, acceleration, planckian transport coefficient, “collapse” to equilibrium, and other bounds in thermal quantum systems,” *Annals of Physics* **443**, 168970 (2022).
- [53] Daniel Louis Jafferis, David K Kolchmeyer, Baur Mukhametzhanov, and Julian Sonner, “Matrix models for eigenstate thermalization,” *arXiv preprint arXiv:2209.02130* (2022).
- [54] Daniel Louis Jafferis, David K Kolchmeyer, Baur Mukhametzhanov, and Julian Sonner, “Jt gravity with matter, generalized eth, and random matrices,” *arXiv preprint arXiv:2209.02131* (2022).
- [55] Jiaozi Wang, Jonas Richter, Mats H Lamann, Robin Steinigeweg, Jochen Gemmer, and Anatoly Dymarsky, “Emergence of unitary symmetry of microcanonically truncated operators in chaotic quantum systems,” *Physical Review E* **110**, L032203 (2024).
- [56] Michele Fava, Jorge Kurchan, and Silvia Pappalardi, “Designs via free probability,” *arXiv preprint arXiv:2308.06200* (2023), 10.48550/arXiv.2308.06200.
- [57] Silvia Pappalardi, Felix Fritzsche, and Tomaz Prosen, “General eigenstate thermalization via free cumulants in quantum lattice systems,” *arXiv preprint arXiv:2303.00713* (2023), 10.48550/arXiv.2303.00713.
- [58] Silvia Pappalardi, Laura Foini, and Jorge Kurchan, “Microcanonical windows on quantum operators,” *Quantum* **8**, 1227 (2024).
- [59] Silvia Pappalardi, Laura Foini, and Jorge Kurchan, “Eigenstate thermalization hypothesis and free probability,” *Phys. Rev. Lett.* **129**, 170603 (2022).
- [60] Dan Voiculescu, “Limit laws for random matrices and free products,” *Inventiones Mathematicae* **104**, 201–220 (1991).
- [61] Dan V Voiculescu, Ken J Dykema, and Alexandru Nica, *Free Random Variables*, 1 (American Mathematical Society, 1992).
- [62] Roland Speicher, “Free probability theory and non-crossing partitions,” *Séminaire Lotharingien de Combinatoire* **39**, B39c–38 (1997).
- [63] Edouard Brézin, Claude Itzykson, Giorgio Parisi, and Jean-Bernard Zuber, “Planar diagrams,” *Communications in Mathematical Physics* **59**, 35–51 (1978).
- [64] Predrag Cvitanović, “Planar perturbation expansion,” *Physics Letters B* **99**, 49–52 (1981).
- [65] Predrag Cvitanović, PG Lauwers, and PN Scharbach, “The planar sector of field theories,” *Nuclear Physics B* **203**, 385–412 (1982).
- [66] Benoît Collins and Ion Nechita, “Random matrix techniques in quantum information theory,” *Journal of Mathematical Physics* **57** (2016).
- [67] Benoît Collins and Ion Nechita, “Random quantum channels i: Graphical calculus and the bell state phenomenon,” *Communications in Mathematical Physics* **297**, 345–370 (2010).
- [68] Jonah Kudler-Flam, Vladimir Narovlansky, and Shinsei Ryu, “Distinguishing random and black hole microstates,” *PRX Quantum* **2**, 040340 (2021).
- [69] Jonah Kudler-Flam, Vladimir Narovlansky, and Shinsei Ryu, “Negativity spectra in random tensor networks and holography,” *Journal of High Energy Physics* **2022**, 1–74 (2022).

- [70] Newton Cheng, Cécilia Lancien, Geoff Penington, Michael Walter, and Freek Witteveen, “Random tensor networks with non-trivial links,” in *Annales Henri Poincaré*, Vol. 25 (Springer, 2024) pp. 2107–2212.
- [71] Ramis Movassagh and Alan Edelman, “Isotropic entanglement,” *arXiv preprint arXiv:1012.5039* (2010).
- [72] Ramis Movassagh and Alan Edelman, “Density of states of quantum spin systems from isotropic entanglement,” *Phys. Rev. Lett.* **107**, 097205 (2011).
- [73] Jiahao Chen, Eric Hontz, Jeremy Moix, Matthew Welborn, Troy Van Voorhis, Alberto Suárez, Ramis Movassagh, and Alan Edelman, “Error analysis of free probability approximations to the density of states of disordered systems,” *Phys. Rev. Lett.* **109**, 036403 (2012).
- [74] Ludwig Hruza and Denis Bernard, “Coherent fluctuations in noisy mesoscopic systems, the open quantum SSEP, and free probability,” *Physical Review X* **13** (2023), 10.1103/physrevx.13.011045.
- [75] Michel Bauer, Denis Bernard, Philippe Biane, and Ludwig Hruza, “Bernoulli variables, classical exclusion processes and free probability,” in *Annales Henri Poincaré* (Springer, 2023) pp. 1–48.
- [76] Denis Bernard and Ludwig Hruza, “Exact entanglement in the driven quantum symmetric simple exclusion process,” *SciPost Physics* **15**, 175 (2023).
- [77] Micha Berkooz, Mikhail Isachenkov, Vladimir Narovlansky, and Genis Torrents, “Towards a full solution of the large  $n$  double-scaled syk model,” *Journal of High Energy Physics* **2019**, 1–72 (2019).
- [78] Geoff Penington, Stephen H Shenker, Douglas Stanford, and Zhenbin Yang, “Replica wormholes and the black hole interior,” *Journal of High Energy Physics* **2022**, 1–87 (2022).
- [79] Jinzhao Wang, “Beyond islands: a free probabilistic approach,” *Journal of High Energy Physics* **2023**, 1–72 (2023).
- [80] Shuang Wu, “Non-commutative probability insights into the double-scaling limit syk model with constant perturbations: moments, cumulants and  $q$ -independence,” *Journal of Physics A: Mathematical and Theoretical* **57**, 325203 (2024).
- [81] Venkatesa Chandrasekaran, Geoff Penington, and Edward Witten, “Large  $n$  algebras and generalized entropy,” *Journal of High Energy Physics* **2023**, 1–68 (2023).
- [82] Giorgio Cipolloni, László Erdős, and Dominik Schröder, “Thermalisation for wigner matrices,” *Journal of Functional Analysis* **282**, 109394 (2022).
- [83] Hyaline Junhe Chen and Jonah Kudler-Flam, “Free independence and the noncrossing partition lattice in dual-unitary quantum circuits,” *arXiv preprint arXiv:2409.17226* (2024).
- [84] F. Haake, M. Kuś, and R. Scharf, “Classical and quantum chaos for a kicked top,” *Z. Phys. B-Condensed Matter* **65**, 381–395 (1987).
- [85] M. Kuś, R. Scharf, and F. Haake, “Symmetry versus degree of level repulsion for kicked quantum systems,” *Zeitschrift für Physik B Condensed Matter* **66**, 129–134 (1987).
- [86] Roberto Benzi, Giovanni Paladin, Giorgio Parisi, and Angelo Vulpiani, “On the multifractal nature of fully developed turbulence and chaotic systems,” *Journal of Physics A: Mathematical and General* **17**, 3521 (1984).
- [87] Giovanni Paladin and Angelo Vulpiani, “Anomalous scaling laws in multifractal objects,” *Physics Reports* **156**, 147–225 (1987).
- [88] Giovanni Paladin and Angelo Vulpiani, “Intermittency in chaotic systems and rényi entropies,” *Journal of Physics A: Mathematical and General* **19**, L997 (1986).
- [89] Andrea Crisanti, Giovanni Paladin, and Angelo Vulpiani, “Generalized lyapunov exponents in high-dimensional chaotic dynamics and products of large random matrices,” *Journal of Statistical Physics* **53**, 583–601 (1988).
- [90] F. Evers and A. D. Mirlin, “Fluctuations of the inverse participation ratio at the anderson transition,” *Phys. Rev. Lett.* **84**, 3690–3693 (2000).
- [91] Nicolas Macé, Fabien Alet, and Nicolas Laflorencie, “Multifractal scalings across the many-body localization transition,” *Phys. Rev. Lett.* **123**, 180601 (2019).
- [92] Piotr Sierant and Xhek Turkeshi, “Universal behavior beyond multifractality of wave functions at measurement-induced phase transitions,” *Phys. Rev. Lett.* **128**, 130605 (2022).
- [93] S. Chaudhury, A. Smith, B. E. Anderson, S. Ghose, and P. S. Jessen, “Quantum signatures of chaos in a kicked top,” *Nature* **461**, 768–771 (2009).
- [94] Qian Wang and Marko Robnik, “Multifractality in quasienergy space of coherent states as a signature of quantum chaos,” *Entropy* **23**, 1347 (2021).
- [95] Silvia Pappalardi, Angelo Russomanno, Bojan Žunkovič, Fernando Iemini, Alessandro Silva, and Rosario Fazio, “Scrambling and entanglement spreading in long-range spin chains,” *Phys. Rev. B* **98**, 134303 (2018).
- [96] Akshay Seshadri, Vaibhav Madhok, and Arul Lakshminarayan, “Tripartite mutual information, entanglement, and scrambling in permutation symmetric systems with an application to quantum chaos,” *Phys. Rev. E* **98**, 052205 (2018).
- [97] Lukas M. Sieberer, Tobias Olsacher, Andreas Elben, Markus Heyl, Philipp Hauke, Fritz Haake, and Peter Zoller, “Digital quantum simulation, trotter errors, and quantum chaos of the kicked top,” *npj Quantum Information* **5** (2019), 10.1038/s41534-019-0192-5.
- [98] Saúl Pilatowsky-Cameo, Jorge Chávez-Carlos, Miguel A. Bastarrachea-Magnani, Pavel Stránský, Sergio Lerma-Hernández, Lea F. Santos, and Jorge G. Hirsch, “Positive quantum lyapunov exponents in experimental systems with a regular classical limit,” *Phys. Rev. E* **101**, 010202 (2020).
- [99] Alessio Lerose and Silvia Pappalardi, “Bridging entanglement dynamics and chaos in semiclassical systems,” *Phys. Rev. A* **102**, 032404 (2020).
- [100] J. M. Deutsch, “Quantum statistical mechanics in a closed system,” *Physical Review A* **43**, 2046–2049 (1991).
- [101] Roland Speicher, “Free probability theory: And its avatars in representation theory, random matrices, and operator algebras; also featuring: Non-commutative distributions,” *Jahresbericht der Deutschen Mathematiker-Vereinigung* **119** (2016), 10.1365/s13291-016-0150-5.
- [102] Xiang-Gen Xia, “A simple introduction to free probability theory and its application to random matrices,” *arXiv preprint arXiv:1902.10763* (2019).
- [103] James A Mingo and Roland Speicher, *Free probability*



- and random matrices*, Vol. 35 (Springer, 2017).
- [104] Noah Linden, Sandu Popescu, Anthony J Short, and Andreas Winter, “Quantum mechanical evolution towards thermal equilibrium,” *Physical Review E—Statistical, Nonlinear, and Soft Matter Physics* **79**, 061103 (2009).
- [105] Yichen Huang, Fernando G. S. L. Brandão, and Yong-Liang Zhang, “Finite-size scaling of out-of-time-ordered correlators at late times,” *Phys. Rev. Lett.* **123**, 010601 (2019).
- [106] Felix Fritzsche and Tomaz Prosen, “Eigenstate thermalization in dual-unitary quantum circuits: Asymptotics of spectral functions,” *Phys. Rev. E* **103**, 062133 (2021).
- [107] Ignacio García-Mata, Marcos Saraceno, Rodolfo A. Jalabert, Augusto J. Roncaglia, and Diego A. Wisniacki, “Chaos signatures in the short and long time behavior of the out-of-time ordered correlator,” *Phys. Rev. Lett.* **121**, 210601 (2018).
- [108] Tomás Notenson, Ignacio García-Mata, Augusto J Roncaglia, and Diego A Wisniacki, “Classical approach to equilibrium of out-of-time ordered correlators in mixed systems,” *Physical Review E* **107**, 064207 (2023).
- [109] Bryce Kobrin, Zhenbin Yang, Gregory D. Kahanamoku-Meyer, Christopher T. Olund, Joel E. Moore, Douglas Stanford, and Norman Y. Yao, “Many-body chaos in the sachdev-ye-kitaev model,” *Phys. Rev. Lett.* **126**, 030602 (2021).
- [110] Joseph Polchinski, “Chaos in the black hole s-matrix,” *arXiv preprint arXiv:1505.08108* (2015).
- [111] Jordan S Cotler, Guy Gur-Ari, Masanori Hanada, Joseph Polchinski, Phil Saad, Stephen H Shenker, Douglas Stanford, Alexandre Streicher, and Masaki Tezuka, “Black holes and random matrices,” *Journal of High Energy Physics* **2017**, 1–54 (2017).
- [112] Luca V Delacretaz, “Heavy operators and hydrodynamic tails,” *SciPost Physics* **9**, 034 (2020).
- [113] Alexander Altland, Dmitry Bagrets, Pranjal Nayak, Julian Sonner, and Manuel Vielma, “From operator statistics to wormholes,” *Phys. Rev. Res.* **3**, 033259 (2021).
- [114] Takato Yoshimura, Samuel J Garratt, and JT Chalker, “Operator dynamics in floquet many-body systems,” *arXiv preprint arXiv:2312.14234* (2023).
- [115] Oscar Bouverot-Dupuis, Silvia Pappalardi, Jorge Kurchan, Anatoli Polkovnikov, and Laura Foini, “Random matrix universality in dynamical correlation functions at late times,” *arXiv preprint arXiv:2407.12103* (2024).